J Therm Anal Calorim (2014) 116:875–879
DOI 10.1007/s10973-013-3568-3

Studies on high-temperature thermal transformation and dielectric property of aluminum–chromium phosphates

Ning Chen · Sijian Gao · Jichuan Huo · Haibin Wang · Jichuan He · Yongchang Zhu

Received: 2 April 2013 / Accepted: 27 November 2013 / Published online: 24 December 2013

Abstract High-temperature thermal transformation of aluminum–chromium phosphates has been investigated by means of DSC–TG, IR, and XRD analysis. The relative dielectric constant and thermal decomposition were measured and discussed. The results show that crystallization and thermal decomposition started at about 1,273 K, only $AlPO_4$ and Cr_2O_3 have been found at 1,873 K due to the decomposition of PO_3^-, $P_2O_7^{2-}$, and PO_4^{3-}. The relative dielectric constant is fluctuant.

Keywords Thermal · Transformation · Phosphate · Binder · Dielectric

Introduction

Al–Cr–phosphate composites have been used as binders in refractory ceramics for many years. It is also well-known that they can be used as a potential wave-transparent material for high-temperature environments because of their low thermal conductivity, low dielectric constant, good chemical stability and high melting point, which are similar to aluminum phosphate binder [1–4]. However, as a high-temperature wave-transparent material, it should also possess a thermally stable dielectric constant [as temperature increases to 373 K, relative dielectric constants (ε_r) change less than 1 %], thermal stability and high thermal shock resistance [5–7]. Han et al. [1, 2, 8] once studied the chemical structure and crystalline phase changes of aluminum–chromium phosphates when cured at temperatures up to 1,473 K. They concluded that a starting phase of the aluminum–chromium phosphates binder is transformed to amorphous at 473 K, and finally to a cyclic $Al(PO_3)_3$ beginning at 973 K. However, the internal structure changes, thermal transformation, thermal decompositions, and relevant dielectric constant at various temperatures have not been investigated. Thus, it is necessary to study the high-temperature thermal transformation and dielectric property of aluminum–chromium phosphates.

In this article, high-temperature thermal transformations of aluminum–chromium phosphates have been studied using thermalgravimetric–differential scanning calorimetry, infrared absorption spectra and X-ray diffraction analysis. The relative dielectric constants (ε_r) were measured using Vector Network Analyzer, and thermal decompositions were discussed through aforementioned analysis.

N. Chen · S. Gao (✉) · Y. Zhu
China Building Materials Academy, Beijing 100024, People's Republic of China
e-mail: gaosijian@263.net

N. Chen
e-mail: xkcn.041@163.com

N. Chen · H. Wang · J. He
Chemistry and Chemical Engineering Institute, Mianyang Normal University, Mianyang 621010, People's Republic of China

J. Huo
Key Laboratory of Nonmetal Composite and Functional Materials of Sichuan Province, Southwest Science and Technology University, Mianyang 621010, People's Republic of China

Experimental

Preparation of samples

Aluminum–chromium phosphates binder was obtained from reagent grade $Al(OH)_3$ (Kelong Chemical, AR), CrO_3

(Galaxy Chemical Co. Ltd., 99 %), and H_3PO_4 (Kelong Chemical, 85 % aqueous solution) using mixing ratio at Al:Cr:P = 3:1:9 (mol%). A typical preparation is described here. 10 g of $Al(OH)_3$ was dissolved in 57.98-g (65 mass%) aqueous H_3PO_4 at 353 K for 30 min until it became clear. Immediately, 4.27 g of CrO_3 was added to the solution, which was quickly dissolved by adding 1.37 g of methanol (Cuicr, AR). The aluminum–chromium phosphates binder obtained is described as the ACP binder. Reaction equations are as follows [3, 8, 9]:

$$Al(OH)_3 + 3H_3PO_4 \xrightarrow{353K} Al(H_2PO_4)_3 + 6H_2O \tag{1}$$

$$Al(H_2PO_4)_3 \xrightarrow{353K} [(H_2PO_4)_2Al(HPO_4)]^- + H^+ \tag{2}$$

$$4CrO_3 + 12[(H_2PO_4)_2Al(HPO_4)]^- + 12H^+ + 3CH_3OH \xrightarrow{353\,K} 4Cr^{3+} + 12[(H_2PO_4)_2Al(HPO_4)]^- + 3HCOOH + 9H_2O \tag{3}$$

$$4Cr^{3+} + 12[(H_2PO_4)_2Al(HPO_4)]^- \xrightarrow{353\,K} 12[(H_2PO_4)_2Al(HPO_4)Cr_{\frac{1}{3}}] \tag{4}$$

Characterization

As the samples were treated at various temperatures, the crystalline phases were identified by means of X-ray diffraction analysis (Model D/max-RB, Rigaku, Japan) between 10° and 80° (2-θ) using a graphite monochromatic Cu Kα radiation, with a step of 0.02° and a scanning rate of 0.5° min^{-1}. Diffraction peaks were indexed with Jade 6 software. Thermal behaviors of specimens were observed using Thermogravimetric analysis–differential scanning calorimetry (TGA–DSC SDT Q600, TA Instrument) with a heating rate ranging from 283 K min^{-1}–1,573 K under dry air. Infrared absorption spectra (AVATAR370, Nicolet, USA) were obtained within the range of 400–4,000 cm^{-1}. The relative dielectric constants (ε_r) were measured within the range of 8–12 GHz at room temperature, using an E5071C vector network analyzer (Agilent).

Results and discussion

Figure 1 shows the XRD patterns of ACP binder with different heat treatments from 293 to 1,873 K. In the samples heated at 1,173 K, there were no obvious crystalline phase but still amorphous. As temperature increased to 1,273 K, amorphous aluminum–chromium phosphates began to crystallize, the dominant phases were $Al(PO_3)_3$,$Cr(PO_3)_3$, and a few $AlPO_4$. After heating up to 1,473 K, the peak intensity of $AlPO_4$ is much more than before with decreasing

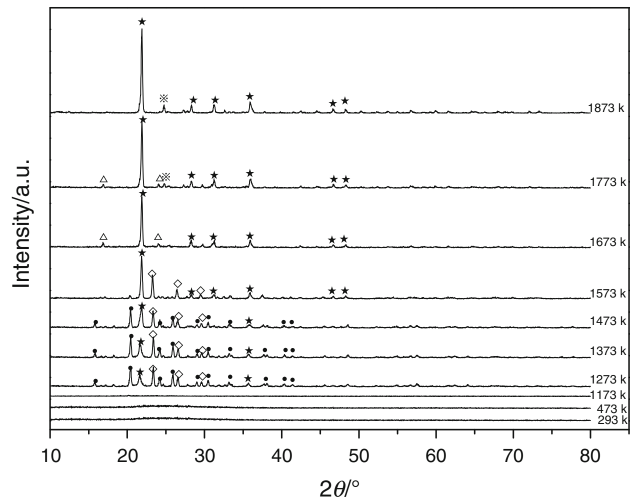

Fig. 1 XRD patterns of ACP binders heated at various temperatures. *Filled circle* $Al(PO_3)_3$, *filled star* $AlPO_4$, *open diamond* $Cr(PO_3)_3$, *open triangle* $Cr_4(P_2O_7)_3$, and ※Cr_2O_3

intensity of $Al(PO_3)_3$ until it completely disappeared at 1,573 K. Based on the analysis from DSC data (seen in Fig. 2), it can be due to the thermal decomposition of $Al(PO_3)_3$. After heating at 1,673 K, the peak of $Cr_4(P_2O_7)_3$ appeared, but $Cr(PO_3)_3$ wasn't detectable. At 1,773 K, Cr_2O_3 was detected by the XRD measurement, and eventually leaving a Cr_2O_3- and $AlPO_4$-rich residue at 1,873 K.

Following a previous study on chromium phosphates' thermal stability [10], the series changes of chromium-containing compound as mentioned above can be ascribed to the thermal decomposition of $Cr(PO_3)_3$ occurring as follows:

$$4Cr(PO_3)_3 \xrightarrow{1673\,K} Cr_4(P_2O_7)_3 + 3P_2O_5\uparrow \tag{5}$$

$$Cr_4(P_2O_7)_3 \xrightarrow{1773-1873\,K} 2Cr_2O_3 + 3P_2O_5\uparrow \tag{6}$$

Figure 2 shows both the DSC and the TG curves of ACP binder from room temperature to 1,573 K. The curves indicated the relationship between temperature change and mass loss of the sample. In the DSC curve, four endothermic stages were recorded with their onset temperatures amounting, respectively, to: 1, 2, 3, and 4, accompanied by varying mass losses. It was observed that the first stage was due to the dehydration and condensation of ACP binder as supported by some earlier studies [8, 11]. The mass loss associated with this endothermic stage was equal to 20 mass%.

For the second endothermic stage, there were no obvious mass loss but a small DTG peak (Fig. 2b). Based on the XRD analysis from 1,173 to 1,273 K, it can be attributed to the complete crystalline transition of amorphous aluminum–chromium phosphates forming metaphosphates like $Al(PO_3)_3$ and $Cr(PO_3)_3$. The small DTG peak is due to the

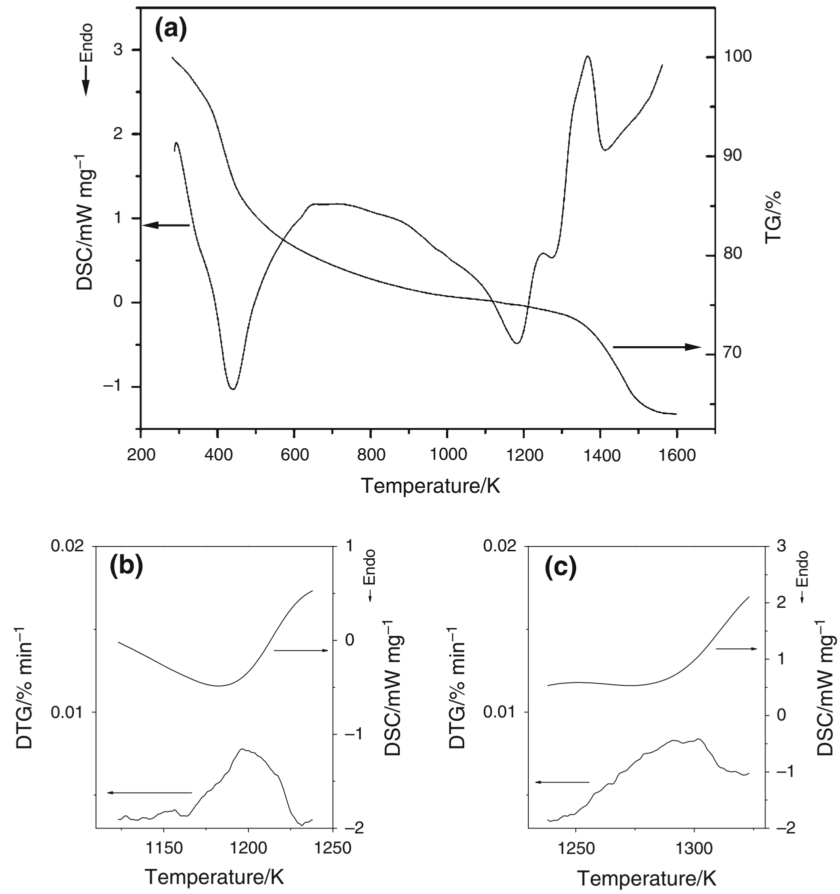

Fig. 2 Thermal analysis curves of ACP binder: **a** DSC–TG patterns of ACP binder; **b** DSC–DTG patterns at the second DSC endothermic stage; **c** DSC–DTG patterns at the third DSC endothermic stage

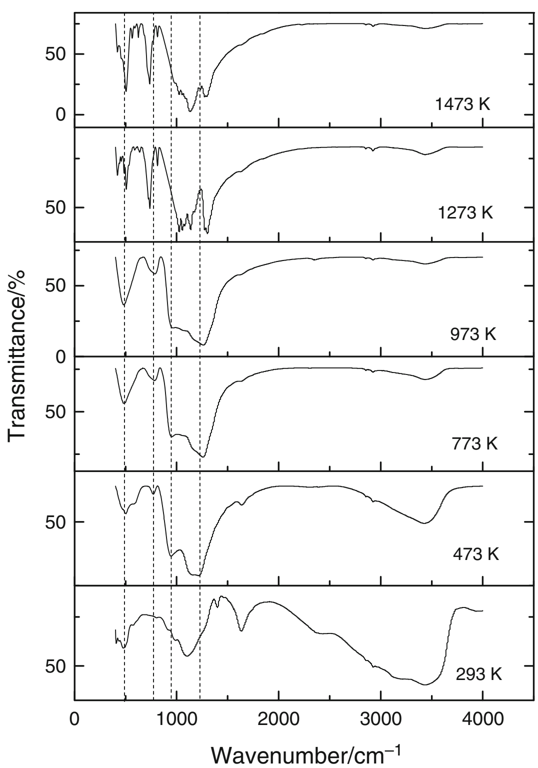

Fig. 3 IR spectra of ACP binders at various temperatures

$Al(PO_3)_3$ decomposition forming $AlPO_4$ and P_2O_5 gas because a few $AlPO_4$ has been detected by XRD measurement, so as to the third endothermic stage (Fig. 2c).

The last endothermic stage, beginning at the onset temperature of 1,423 K, is accompanied by a wide mass loss. Considering the XRD analysis from 1,373 to 1,573 K, it can be concluded that these endothermic and mass losses are associated with the complete decomposition of $Al(PO_3)_3$ that takes place probably according to the equations [11–14]:

$$Al(PO_3)_3 \xrightarrow{1473-1573\ K} AlPO_4 + P_2O_5 \uparrow \quad (7)$$

The IR spectra of ACP binder between 293 and 1,473 K are given in Fig. 3. Five infrared absorption bands at 1240, 1097, 940, 776 cm and 480 cm^{-1} gradually changed with high-temperature treatment. The 1,097 cm^{-1} band is converted to broad absorption band in the range 1,240–940 cm^{-1}, after 473 K heating. Then, the 1,240 cm^{-1} band (bridging O=P–O) shifts up to 1,280 cm^{-1}, the absorption maximum at 940 cm^{-1} (P–O–P) moves to 1,150 cm^{-1} (Al–O–P). Simultaneously, the 776-cm^{-1} band moves right with the increasing intensity.

IR reflectance spectra of $Al(H_2PO_4)_3$ and ACP binder have been reported by Waleed Mekky [10] and Han et al. [4]. Their spectra show the same trend. Following the

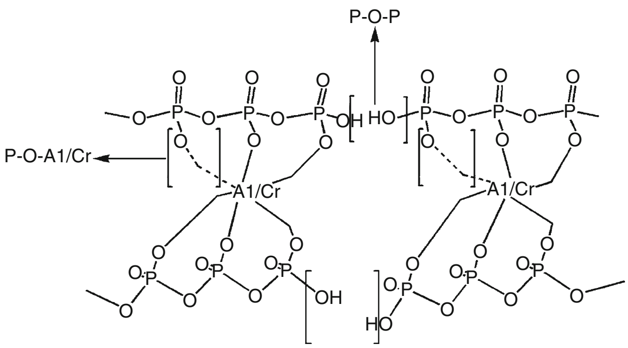

Fig. 4 Schematic representation of internal condensation reaction of amorphous aluminum–chromium phosphates

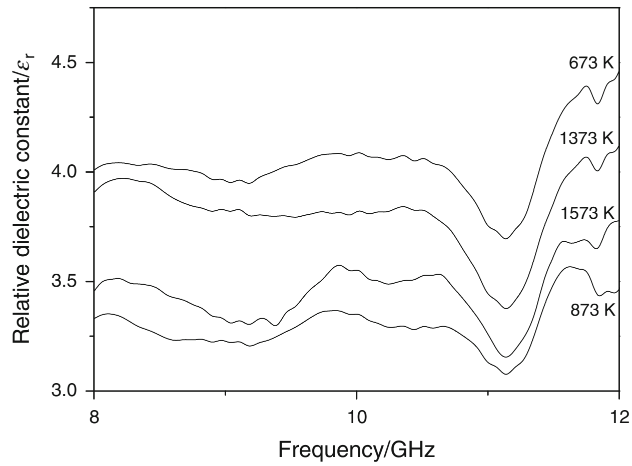

Fig. 5 Relationship between wave frequency and relative dielectric constants (ε_r) of ACP binder heated at various temperatures

numerous spectral studies on phosphate [15–28], the bands observed can be assigned as follows. The principal band at 1,240 cm^{-1} in the IR spectra is due to the asymmetric stretching of bridging PO_2 (O=P–O–Al/Cr), the observed band in 1,097 cm^{-1} are attributed to the PO_4^{3-} bending and stretching vibrations. Bands at 1,150 and 1,280 cm^{-1} was assigned to the stretching vibration of PO_3 groups. In addition, bands at 940 and 776 cm^{-1} belong to the asymmetric stretching vibration of the linear P–O–P chain.

After heating at 473 K, the band at 1,097 cm^{-1} disappeared, converting to broad absorption band in the range 1,240–940 cm^{-1} with the vast decreasing intensity of the hydroxyl group, –OH, at 1,638 cm^{-1}. It can be attributed to the transformation of dihydric phosphates to polymerized Phosphates, a condensation reaction between P–OH and P–OH. From temperatures 473 to 973 K, the bands at 776 and 1,240 cm^{-1} gradually increased with decreasing intensity of the hydroxyl group, –OH, at 1,638 and 3,467 cm^{-1}, respectively. This was presumably due to an internal condensation reaction of amorphous aluminum–chromium phosphates, condensation reactions between O=P–OH and –O–Al/Cr–O–, P–O–P–OH and P–O–P–OH. Figure 4 shows the reactions with a simple model of aluminum phosphate glasses [29–31]. In this figure, hydroxyl groups, P–O–P–OH, polymerized to form longer linear P–O–P chain, O=P–OH and –O–Al/Cr–O– groups polymerized to form more bridging PO_2 (O=P–O–Al/Cr), finally, the bridging of the chains and three-dimensional structures of amorphous aluminum–chromium phosphates have been strengthened. Moreover, this fact is also confirmed by DSC-TG and dielectric constant testings. Because of the water losing constantly in those condensation reactions, the dielectric constant (seen in Fig. 5) and TG curve (seen in Fig. 2) decreased below 1,073 K. After 1,273 K thermal treatment, 776-, 940-, and 1,240-cm^{-1} bands, respectively, are converted into three new sharp absorption peaks, 750, 1150, and 1280 cm^{-1}. The appearance of these new bands, which was assigned to the asymmetric stretch of the P–O–P and PO_2 rings, suggests that the P–O–P and O=P–O bonds began to change from a linear or bridging structure to a small (three- or four-member) metaphosphate $Al(PO_3)_3$ ring structure. This also can be confirmed by means of XRD patterns at 1,273 K.

Figure 5 shows the relationship between the heating temperature and the relative dielectric constants with different temperature treatments. The data reveal a fluctuant dielectric constant with the increasing heating temperature. For instance, at 10 GHz, the dielectric constant of the sample drops from 4.2 to 3.3 when temperature increases from 673 to 873 K, but increases to 3.8 when temperature increases to 1,373 K, and finally decreases to 3.5 at 1,573 K. The decrease in dielectric constant from 673 to 873 K is possibly related to the further internal condensation dehydration of amorphous aluminum–chromium phosphates. The increase in dielectric constant to 1,373 K is probably due to the metaphosphate phase formed from amorphous phase which has a higher electric dipole moment. This leads to the increase of ionic polarizability which is the key factor affecting the dielectric constant. The last decrease in dielectric constant to 1,573 K is attributed to the thermal decomposition from $Al(PO_3)_3$ to $AlPO_4$ because of a lower refractive index than that of the metaphosphate [32].

Conclusions

The results of the conducted research allow for the following statements:

- About 443 K, the starting phase of the ACP binder transformed to amorphous via condensation.
- At temperatures from 473 to 1,173 K, the only phase is amorphous. However, IR and DSC–TG analyses show that amorphous structure is variational: residual

hydroxyl groups, P–O–P–OH polymerized to form longer linear P–O–P chain, and O=P–OH and Al/Cr–OH groups polymerized to form more bridging PO_2 (O=P–O–Al/Cr).

- Approximately at 1,273 K, amorphous phase began to crystallize, forming metaphosphates like $Al(PO_3)_3$ and $Cr(PO_3)_3$.
- At 1,473 K, $Al(PO_3)_3$ began to decompose into $AlPO_4$ and P_2O_5 gas according to Eq. (7).
- Between 1,673 and 1,873 K, $Cr(PO_3)_3$ has undergone two decompositions, first, forming $Cr_4(P_2O_7)_3$ and P_2O_5 gas, and then transforming into Cr_2O_3 and P_2O_5 gas according to Eqs. (5) and (6).
- Thermal transformation of Aluminum–chromium Phosphates from 473 to 1,873 K lead to a fluctuant dielectric constant, but finally stabled at 3–4 because of the final products $AlPO_4$ and Cr_2O_3.

Acknowledgements The authors acknowledged the financial supports from the National High Technology Research and Development Program of China (863 Program No. 2009AA035002), the Foundation of Sichuan Educational Committee of China (No. 10ZA061, No. 13ZB0117).

References

1. Hong LY, Han HJ, Ha H, Lee JY, Kim DP. Development of Cr-free aluminum phosphate binders and their composite applications. Comput Sci Technol. 2007;67:1195–201.
2. Kim DP, Myung HS, Rho JS, Han KS, Woo HG, Ha H, Cao F. Fabrication and properties of thermal insulating glass fiber reinforced composites from low temperature curable polyphosphate inorganic polymers. Comput Sci Technol. 2003;63:493–9.
3. Gutiérrez Mora F, Goretta KC, Singh D, Routbort JL, Sambasivan S, Steiner KA, Adabie J, Rangan KK. High-temperature deformation of amorphous $AlPO_4$-based nano-composites. J Eur Ceram Soc. 2006;26:1179–83.
4. Liu ZH, Huo JC, Wang HB, Lei H, Lei YL. The effect of fillers on chrome-based wave-transparent material matrix. Adv Mater Res. 2012;557:357–61.
5. Ganesh I. Development of β-SiAlON based ceramics for radome applications. Process Appl Ceram. 2011;5:113–38.
6. Wang Y, Liu J. Aluminum phosphate–mullite composites for high-temperature radome applications. Int J Appl Ceram Technol. 2009;6:190–4.
7. Ganesh I, Thiyagarajan N, Jana DC, Mahajan YR, Sundararajan G. Aqueous gelcasting process for β-$Si_4Al_2O_2N_6$ ceramics. J Am Ceram Soc. 2008;91:3121–4.
8. Han HJ, Kim DP. Studies on curing chemistry of aluminum–chromium–phosphates as low temperature curable binders. J Sol–Gel Sci Technol. 2003;6:223–8.
9. Tricot G, Coillot D, Creton E, Montagne L. New insights into the thermal evolution of aluminophosphate solutions A complementary XRD and solid state NMR study. J Eur Ceram Soc. 2008;6:1135–41.
10. Bosacka M, Jakubus P, Himmel IR. Obtaining of chromium(III) phosphates(V) in the solid-state and their thermal stability. J Therm Anal Calorim. 2007;88:133–7.
11. Chao L, Lei Z, Zhou K, Li Z, Zi C. Interface microstructure and bonding mechanism of phosphate bonding $NiFe_2O_4$ cermet. Chin J Nonferrous Met. 2011;21:1060–5.
12. Wang J. Preparation, microstructure and properties of lightweight Al_2O_3 bubble ceramic. Zhejiang: Zhejiang University; 2002.
13. Liyun C, Qun M, Jianfeng H, Xinping Y. Influence of hydrothermal treatment temperature on oxidation modification of C/C composites with aluminum phosphates solution by a microwave hydrothermal process. Corros Sci. 2010;52:3757–62.
14. Cinausero N, Azema N, Lopez-Cuesta J-M, Cochez M, Ferriol M. Synergistic effect between hydrophobic oxide nanoparticles and ammonium polyphosphate on fire properties of poly(methyl methacrylate) and polystyrene. Polym Degrad Stab. 2011;96:1445–54.
15. Mekky W, Nicholson PS. Nano-aluminum–phosphate via a polymerized organic–inorganic complex route. J Mater Process Technol. 2007;190:393–6.
16. Baran J, Trzebiatowska M, Ratajczak H. Polarised IR and Raman spectra of monoglycine dihydrogenphosphate single crystal. J Mol Struct. 2004;708:127–44.
17. Byrappa K, Srikantaswamy S, Gopalakrishna GS, Ven Katach Alapathy V. Infrared spectra of aluminum orthophosphate crystals. J Mater Sci Lett. 1986;5:203–5.
18. Karabulut M, Metwalli E, Brow RK. Mechanical and structural properties of lanthanum–aluminum–phosphate glasses. J Non-Cryst Solids. 2001;283:211–9.
19. Karabulut M, Metwalli E, Stefan R, Marasinghe GK, Ray CS, Kurkjian CR, Day DE. Mechanical and structural properties of phosphate glasses. J Non-Cryst Solids. 2001;288:8–17.
20. Karabulut M, Yuce B, Bozdogan O, Ertap H, Mammadov GM. Effect of boron addition on the structure and properties of iron phosphate glasses. J Non-Cryst Solids. 2011;357:1455–62.
21. Onoda H, Sakai R, Nakahira A, Tanaka I. Synthesis of porous aluminum phosphate bulks by hydrothermal hot pressing process and their analytical characterizations. Inorg Mater. 2009;45:1048–52.
22. Xie W, Yang D. Transesterification of soybean oil over WO_3 supported on $AlPO_4$ as a solid acid catalyst. Bioresour Technol. 2012;119:60–5.
23. Mošner P, Vosejpková K, Koudelka L, Beneš L. Thermal studies of $ZnO–B_2O_3–P_2O_5–TeO_2$ glasses. J Therm Anal Calorim. 2012; 107:1129–35.
24. Boonchom B, Youngme S, Srithanratana T, Danvirutai C. Synthesis of $AlPO_4$ and kinetics of thermal decomposition of $AlPO_4{\cdot}H_2O–H_4$ precursor. J Therm Anal Calorim. 2008;91:511–6.
25. Boonchom B, Kongtaweelert S. Study of kinetics and thermodynamics of the dehydration reaction of $AlPO_4{\cdot}$ H_2O. J Therm Anal Calorim. 2010;99:531–8.
26. Boonchom B, Vittayakorn N. Dehydration behavior of synthetic $Al_{0.5}Fe_{0.5}PO_4$ $\cdot 2.5H_2O$. J Chem Eng Data. 2010;55:3307–11.
27. He Y, Liao S, Chen Z, Yu L, Xia Y, Wenwei W, Li B. Non-isothermal kinetics study with isoconversional procedure and DAEM: $LiCoPO_4$ synthesized from thermal decomposition of the precursor. Ind Eng Chem Res. 2013;52:1870–6.
28. Chen Z, Chai Q, Liao S, He Y, Wu W, Li B. Preparation of LiZnPO4 H_2O via a novel modified method and its non-isothermal kinetics and thermodynamics of thermal decomposition. J Therm Anal Calorim. 2012;108:1235–42.
29. Schneider J, Oliveira SL, Nunes LO, Panepucci H. Local structure of sodium aluminum metaphosphate glasses. J Am Ceram Soc. 2003;86:317–24.
30. James Kazama J. Oral phosphate binders: history and prospects. Bone. 2009;45:S8–12.
31. Tsuchida J, Schneider J, Rinke MT, Eckert H. Structure of ternary aluminum metaphosphate glasses. J Phys Chem C. 2011;115: 21927–41.
32. Kolb ED, Glass AM, Rosenberg RL, Grenier JC, Laudise RA. Dielectric and piezoelectric properties of aluminum phosphate. Albany: IUS; 1981. p. 332–6.